

Perturbations of Q-balls: from spectral structure to radiation pressure

Dominik Ciurla,^{a,d} Patrick Dorey,^b Tomasz Romańczukiewicz^a and Yakov Shnir^c

^a*Faculty of Physics, Astronomy and Applied Computer Science, Jagiellonian University, Kraków, Poland*

^b*Department of Mathematical Sciences, Durham University, Durham DH1 3LE, UK*

^c*Institute of Physics, University of Oldenburg, Oldenburg D-26111, Germany
Hanse-Wissenschaftskolleg, Lehmkuhlenbusch 4, 27733 Delmenhorst, Germany*

^d*Doctoral School of Exact and Natural Sciences, Jagiellonian University, Kraków, Poland*

E-mail: dominik.ciurla@doctoral.uj.edu.pl, p.e.dorey@durham.ac.uk,
tomasz.romanczukiewicz@uj.edu.pl, shnir@maths.tcd.ie

ABSTRACT: We investigate Q-balls in a 1+1 dimensional complex scalar field theory. We find that the relaxation of a squashed Q-ball is dominated by the decay of a normal mode through nonlinear coupling to scattering modes and a long-lasting quasi-normal mode. We also study how these Q-balls behave when exposed to scalar radiation, finding that for certain conditions they can experience negative radiation pressure.

Contents

1	Introduction	1
2	A class of Q-balls in 1+1 dimensions	2
2.1	The model	2
2.2	Stationary solutions	4
3	Spectral structure	5
3.1	Linearization	5
3.2	Zero modes	6
3.3	Half-propagating and quasi-normal modes	8
3.4	Bound modes	9
3.5	Mode decay	10
4	Radiation pressure	13
5	Conclusions	15
A	Metastable Q-balls	17

1 Introduction

Q-balls are non-topological solitons which arise in various non-linear scalar field theories possessing an unbroken continuous global symmetry [1–3]. They carry a Noether charge associated with this symmetry, and are stationary localized field configurations with an explicitly time-dependent phase. Typical examples of Q-balls in flat 3+1 dimensional Minkowski spacetime are spherically symmetric solutions of a model with a single complex scalar field and a suitable self-interaction potential [3], or solitons of the renormalizable Friedberg-Lee-Sirlin two-component model with a symmetry breaking potential [2]. Physically, they can be considered as a condensate of a large number of scalar quanta which, for a fixed value of the charge Q , yields an extremum of the effective energy functional. In such a context, the charge can also be interpreted as the particle number.

Q-balls have received considerable attention over the last three decades (for a review, see, e.g., [4–6]). However, most works address the stability of stationary Q-balls and the domains of their existence. There have only been a few studies of the dynamics of Q-balls [7–10], which appears to be very different from the usual dynamics of topological solitons. The reasons for this are related to phase-dependent force of interaction between the Q-balls, their non-topological charge which can be transferred in collisions [10], and the complicated spectrum of their excitations, which as we will show below may include both normal and

quasinormal (QNM) modes (for discussions of QNM see [11–13] in the context of black holes, [14] in relation with excitations of a non-Abelian monopole, and [15]). Furthermore, in some cases these excitations cannot be considered as linearized perturbations, since at least second order corrections must be taken into account in order to understand them fully [16].

There is some similarity between Q-balls and oscillons [17–19], extremely long-lived, spatially localized, almost periodic non-linear field configurations. It was pointed out that a Q-ball can be roughly viewed as a system of two interacting oscillons, associated with real components of a complex scalar field [10]. However, while Q-balls are non-radiating stationary solutions, oscillons slowly radiate energy [20–22]. A peculiar feature of the radiation of an oscillon is its resonant character [23–25]: the radiating oscillon can pass through a sequence of quasi-stable Q-ball-like configurations. The relation between Q-balls and oscillons is supported by the existence of a so-called adiabatic invariant that is approximately conserved [26–28].

Important information about the properties of solitons can be obtained from the study of their interactions with external perturbations. In particular, one can consider a small amplitude incoming wave moving towards a soliton. It has been observed that in a large class of models with kink solutions the radiation pressure exerted on the kink can be negative [29–31]. Similar effects were found in Bose-Einstein condensates [32]. Scalar radiation may also strongly influence the dynamics of soliton collisions [33], so a natural question arises as to what the effect of the interaction of Q-balls with incoming scalar radiation might be.

In simple cases in (1+1) dimensions, analytical solutions for stationary Q-balls are known, as discussed, for example, in [9]. The goal of this paper is to study perturbative excitations of some of these Q-balls. In particular, we reconsider squashing perturbations of a single Q-ball [9] and examine the effects of radiation pressure. The paper is organized as follows. In section 2, we define the model and some important properties of the Q-balls. Section 3 is devoted to the linearization problem and spectral structure of the Q-balls. We analyze scattering and bound modes, as well as the so-called half-propagating modes, investigating in particular their connection with quasinormal modes. We analyze how the spectral structure, and especially the bound and quasinormal modes, influences the long-term evolution of a perturbed Q-ball. In section 4, we focus on the motion of Q-balls interacting with a monochromatic wave. We find that for a certain set of parameters, it is possible for Q-balls to accelerate towards the source of radiation, which is an indication of the negative radiation pressure. After our conclusions in section 5, we comment in appendix A on the results of [9] for a metastable Q-ball.

2 A class of Q-balls in 1+1 dimensions

2.1 The model

The (1+1)-dimensional scalar field theory we will study is defined by the following Lagrangian [7, 9]:

$$\mathcal{L} = \partial_\mu \phi \partial^\mu \phi^* - V(|\phi|^2) , \quad (2.1)$$

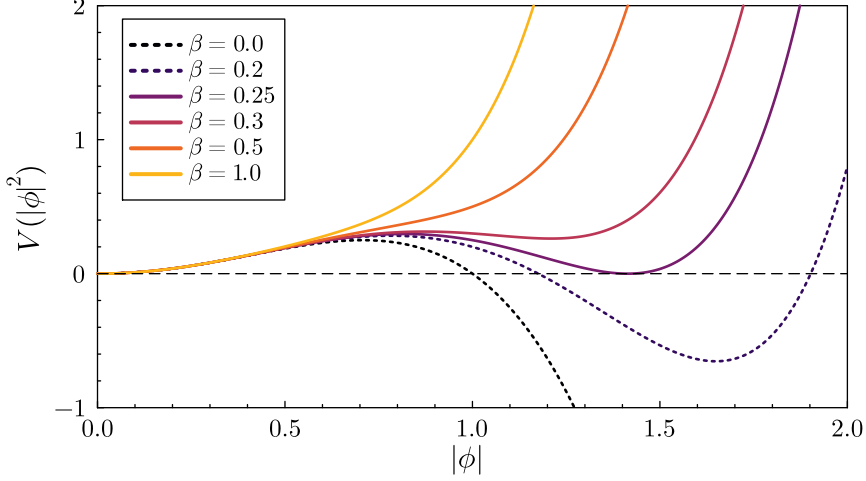


Figure 1. The field theory potential $V(|\phi|^2)$ defined by (2.2) for various values of β . For the potentials shown with dotted lines, the vacuum at $|\phi| = 0$ is metastable.

where the asterisk denotes complex conjugation and the rescaled potential of the self-interacting complex scalar field ϕ is

$$V(|\phi|^2) = |\phi|^2 - |\phi|^4 + \beta|\phi|^6. \quad (2.2)$$

This potential is shown for various values of the parameter β in figure 1. There is a minimum at $\phi = 0$ which for $\beta > 1/4$ is the global minimum, while for $\beta < 1/3$ there is a second minimum at $|\phi|^2 = 1 + \sqrt{1 - 3\beta}$.

The global $U(1)$ symmetry of the Lagrangian (2.1) corresponds to the conserved current

$$j_\mu = i(\phi^* \partial_\mu \phi - \partial_\mu \phi^* \phi), \quad \partial^\mu j_\mu = 0. \quad (2.3)$$

Variation of the Lagrangian (2.1) with respect to the scalar field leads to the equation of motion

$$\phi_{tt} - \phi_{xx} + \frac{\partial V}{\partial |\phi|^2} \phi = 0 \quad (2.4)$$

A stationary (1+1)-dimensional Q-ball configuration with harmonic time dependence can be parameterised as

$$\phi(x, t) = e^{i\omega t} f(x) \quad (2.5)$$

where $f(x)$ is a real profile function which satisfies the first order equation

$$\frac{df}{dx} = \pm \sqrt{\tilde{V}(f^2)} \quad (2.6)$$

with the boundary conditions $f(\pm\infty) = 0$, and

$$\tilde{V}(f^2) = V(f^2) - \omega^2 f^2 \quad (2.7)$$

is the effective potential for the Q-ball configuration. Further specifying $f_x(0) = 0$ centres the profile function on the origin.

The Noether charge of the stationary configuration is

$$Q = \int dx j_0 = 2\omega \int dx f^2 = 2\omega N, \quad (2.8)$$

where N is the L^2 norm of the scalar field. The total energy of the Q-ball can be written as

$$E = \int dx \left\{ (f_x)^2 + \omega^2 f^2 + V(f^2) \right\} = \int dx \left\{ (f_x)^2 + \tilde{V}(f^2) \right\} + \omega Q. \quad (2.9)$$

2.2 Stationary solutions

Equation (2.6) admits the analytic solution

$$f(x; \omega) = \frac{\sqrt{2}\omega'}{\sqrt{1 + \sqrt{1 - 4\beta\omega'^2} \cosh(2\omega'x)}}, \quad (2.10)$$

where $\omega' = \sqrt{1 - \omega^2}$ is the complementary frequency [9]. For the sake of simplicity, we will drop ω and write a shorthand version $f(x)$ in most cases, except for one paragraph in section 3.2.

Localized soliton solutions of the model (2.1) exist only for a limited range of values of the angular frequency, $\omega_{\min} \leq \omega \leq \omega_{\max}$. Here the upper bound corresponds to mass of the linearized scalar excitations, $\omega_{\max} = V''(0)/2 = 1$, and the lower bound depends on the value of the parameter β as [9]

$$\omega_{\min}(\beta) = \sqrt{1 - \frac{1}{4\beta}}. \quad (2.11)$$

Note that the potential (2.2) possesses a unique global minimum at $\phi = 0$ if $\beta > \frac{1}{4}$. If $\beta < \frac{1}{4}$, the local minimum at $\phi = 0$ becomes a false vacuum. In such a case, the configuration (2.10) will be metastable. Finally, in the marginal case $\beta = \frac{1}{4}$ the vacuum $V(|\phi|^2) = 0$ is two-fold degenerate between $\phi_0 = 0$ and $|\phi_1| = \sqrt{2}$ and the model supports topological solitons, or kinks. In this limit, the minimal value of the angular frequency is zero.

More generally, as the angular frequency approaches the minimal value ω_{\min} (2.11), the effective potential $\tilde{V}(f^2)$ takes the form of the standard ϕ^6 potential

$$\tilde{V}(f^2) = \beta f^2 \left(f^2 - \frac{1}{2\beta} \right)^2 \quad (2.12)$$

with minima at $\tilde{V}(0) = \tilde{V}\left(\frac{1}{2\beta}\right) = 0$ and the Q-ball splits into a pair of kink-like solutions interpolating between these vacua [34]

$$\phi_K(x, t) = \frac{e^{i\omega_{\min}t}}{2\sqrt{\beta}} \sqrt{1 \pm \tanh\left(\frac{x}{2\sqrt{\beta}}\right)}. \quad (2.13)$$

The energy of a kink is $E_K = \frac{1}{8}\beta^{-3/2}$.

Substitution of the ansatz (2.10) into expressions (2.8) and (2.9) for the energy and the charge of the configuration gives [9]

$$E = \frac{4\omega\omega' + Q(4\beta - 1 + 4\beta\omega^2)}{8\omega\beta}; \quad Q = \frac{4\omega}{\sqrt{\beta}} \operatorname{arctanh} \left(\frac{1 - \sqrt{1 - 4\beta\omega'^2}}{2\omega'\sqrt{\beta}} \right). \quad (2.14)$$

Note, it is possible to consider Q-balls for $\beta < \frac{1}{4}$, but in such cases they are excitations of a false vacuum and are only metastable solutions. Large perturbations can lead to a collapse to a true vacuum. In [9] the authors considered a relaxation process of a weakly perturbed Q-ball for $\beta = 0$. In this paper we will mostly assume that $\beta > \frac{1}{4}$, although some results for $\beta = 0$ will be discussed in the Appendix.

3 Spectral structure

3.1 Linearization

Our aim now is to analyse the spectrum of linearized perturbations of these Q-balls. By analogy with the analysis of stability of the solutions in [16, 35], we consider a perturbative expansion of the scalar field

$$\phi(x, t) = f(x)e^{i\omega t} + A\xi(x, t) + \dots, \quad (3.1)$$

where the real parameter A is the amplitude of the small perturbation of the Q-ball, and substitute it into the field equation (2.4). In the linear approximation in A we obtain

$$\ddot{\xi} - \xi'' + [V'(f^2) + V''(f^2)f^2]\xi + V''(f^2)f^2\xi^* = 0. \quad (3.2)$$

For oscillating modes it is consistent to consider perturbations ξ of the form

$$\xi(x, t) = e^{i(\omega+\rho)t}\eta_1(x) + e^{i(\omega-\rho)t}\eta_2(x), \quad (3.3)$$

where the parameter ρ encodes the possible eigenfrequencies of the perturbation. The linearized equation (3.2) can then be written as a set of two coupled second order ordinary differential equations for the components η_1 and η_2^* :

$$L \begin{bmatrix} \eta_1 \\ \eta_2^* \end{bmatrix} = 0 \quad (3.4)$$

$$L = - \begin{bmatrix} (\omega + \rho)^2 & \\ & (\omega - \rho)^2 \end{bmatrix} + \begin{bmatrix} D & S \\ S & D \end{bmatrix} \quad (3.5)$$

where

$$D = -\frac{d^2}{dx^2} + U + S \quad (3.6)$$

and the potentials of perturbations $U(x)$ and $S(x)$ are (see Figure 2)

$$U = V'(f^2) = 1 - 2f^2 + 3\beta f^4 \quad (3.7)$$

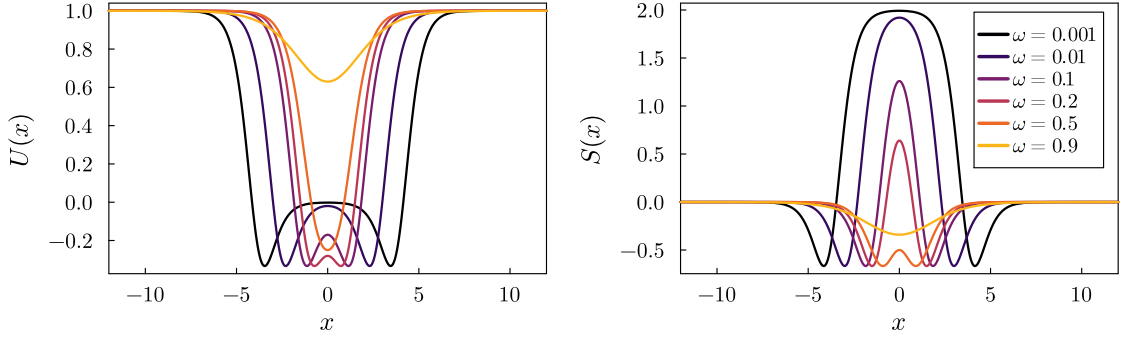


Figure 2. Potentials of linearized perturbations $U(x)$ and $S(x)$, defined in equations (3.7) and (3.8), for selected values of ω and $\beta = \frac{1}{4}$.

$$S = f^2 V''(f^2) = f^2(-2 + 6\beta f^2) \quad (3.8)$$

Note that $U(x) \rightarrow 1$ and $S(x) \rightarrow 0$ as $|x| \rightarrow \infty$. In these limits the equations for η_1 and η_2 decouple.

Assuming $\omega > 0$, we consider the following cases:

- $\rho \in (0, 1 - \omega)$: there are no traveling waves, however, bound modes may exist, depending on the form of the potential.
- $\rho \in (1 - \omega, 1 + \omega)$: only the component η_1 is asymptotically propagating, with $e^{-ik_1 x}$ the right-moving mode and $e^{ik_1 x}$ the left-moving mode, where the wavenumber is $k_1 = \sqrt{(\omega + \rho)^2 - 1} > 0$. The second component η_2 remains exponentially localized on the Q-ball, $k_2^2 = (\omega - \rho)^2 - 1 < 0$. Throughout this paper we will refer to this state as the half-propagating mode. Such modes are crucial for understanding quasinormal modes in other models, including the 't Hooft-Polyakov monopole [14].
- $\rho > 1 + \omega$: both components are propagating, but the component η_2 oscillates with *negative* frequency, which means that for $k_2 > 0$ the term $e^{ik_2 x}$ describes a wave moving to the right, $k_2 = \sqrt{(\omega - \rho)^2 - 1} > 0$. An example of such a mode is presented in figures 3 and 4.

3.2 Zero modes

There are two zero modes that satisfy the equation (3.4) with $\rho = 0$. One of them is the translational mode, which shifts the position of the Q-ball,

$$\eta_0^{(tr)}(x) = \partial_x f(x); \quad (f(x) - x_0 \eta_0^{(tr)}(x)) e^{i\omega t} \approx f(x - x_0) e^{i\omega t}. \quad (3.9)$$

The other one is the phase shifting zero mode

$$\eta_0^{(ph)}(x) = f(x); \quad (f(x) + i\alpha \eta_0^{(ph)}(x)) e^{i\omega t} \approx f(x) e^{i\omega t + i\alpha}, \quad (3.10)$$

which corresponds to the global $U(1)$ symmetry of the model (2.1).

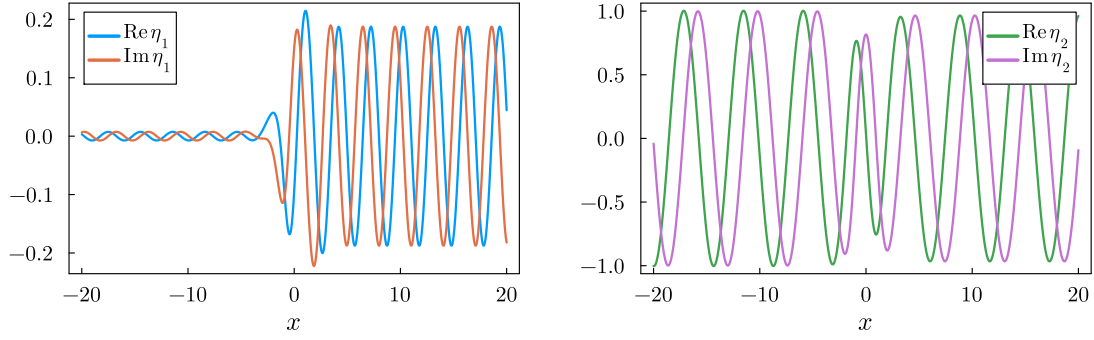


Figure 3. Example solution to the linearized problem for $\beta = \frac{1}{4}$, $\omega = 0.8$ and $\rho = 2$ with a wave travelling to the right in the second channel.

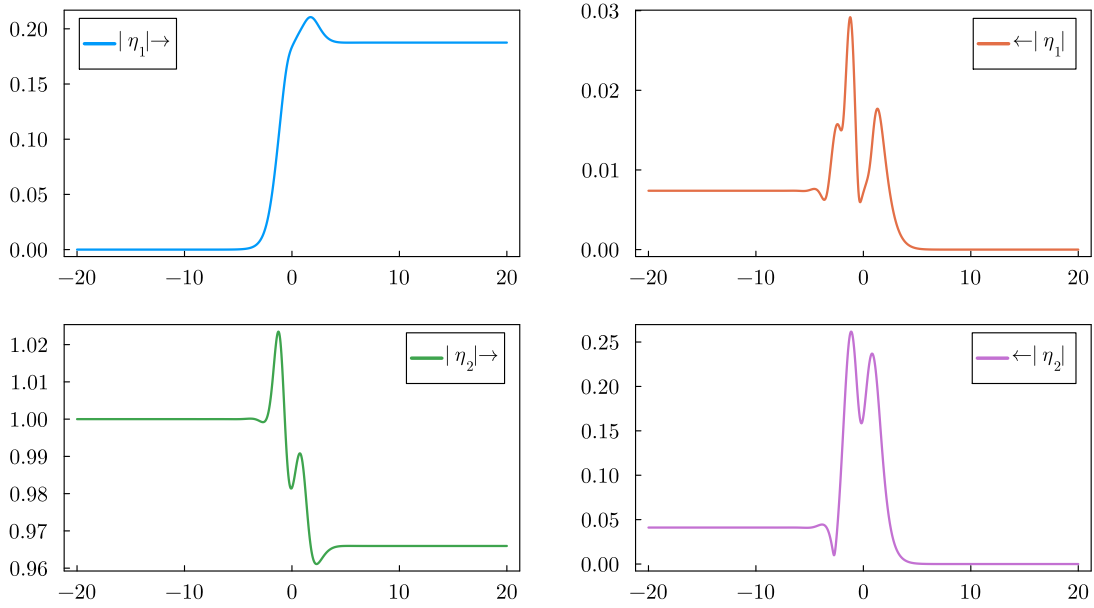


Figure 4. Decomposition of the wave into scattered components for $\beta = \frac{1}{4}$, $\omega = 0.8$ and $\rho = 2$ with a wave travelling right boundary conditions

However, apart from these two modes, there are two more solutions of the linearized equation (3.2), of the form $\xi(x, t) = \eta(x, t)e^{i\omega t}$ with the η factor also time dependent: a stationary mode $\eta^{(Q)}(x, t)$, which transforms the frequency of the Q-ball ω as $\omega + \delta\omega$, and a mode corresponding to Lorentz symmetry. Recall that the profile function $f(x; \omega)$ (2.10) depends on the frequency, therefore excitation of this mode affects both the frequency and the profile of the Q-ball, thus

$$\eta^{(Q)}(x, t) = \partial_\omega f(x; \omega) + itf(x; \omega); \quad (f(x; \omega) + \delta\omega\eta^{(Q)}(x, t))e^{i\omega t} \approx f(x; \omega + \delta\omega)e^{i(\omega + \delta\omega)t}. \quad (3.11)$$

The Lorentz symmetry mode is

$$\eta^{(Lor)}(x, t) = t\partial_x f(x) + i\omega x f(x), \quad (3.12)$$

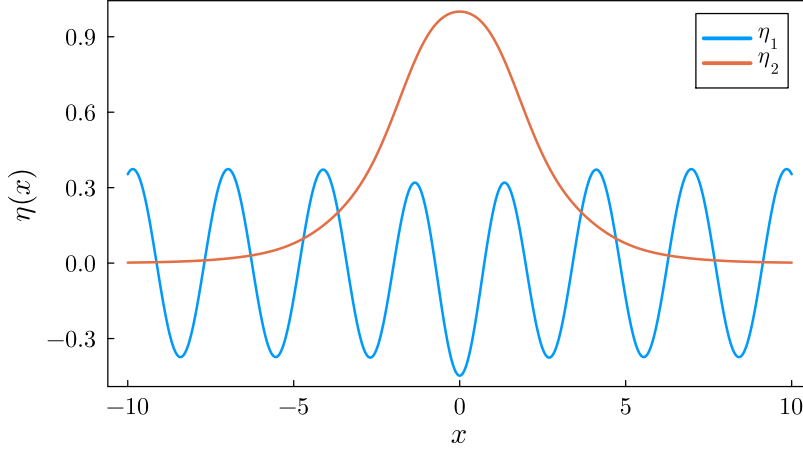


Figure 5. An example of symmetric half-propagating mode for $\beta = \frac{1}{4}$ and $\omega = \frac{\sqrt{3}}{2}$, $\rho = 1.54$.

which follows from the expansion of a boosted Q-ball solution expanded up to $\mathcal{O}(v)$ terms:

$$f(\gamma(x - vt))e^{i\gamma\omega(t-vx)} \approx [f(x) - v(t\partial_x f(x) + i\omega x f(x))]e^{i\omega t}. \quad (3.13)$$

Note that translational, phase shifting and Lorentz zero modes preserve the charge of the Q-ball while the frequency transforming mode changes it.

3.3 Half-propagating and quasi-normal modes

For ρ within the range $(1 - \omega, 1 + \omega)$ only one component of the linearized solution propagates, $k_1^2 > 0$, whereas the other component cannot, $k_2^2 < 0$. In such a case, the second component η_2 has to decay as $x \rightarrow \pm\infty$, as $e^{\mp|k_2|x}$.

In our numerical calculations we fixed

$$\eta'_1(0) = \eta'_2(0) = 0 \quad (3.14a)$$

for a symmetric solution, normalised by setting

$$\eta_2(0) = 1, \quad (3.14b)$$

and then adjusted the value of $\eta_1(0)$ so as to satisfy the remaining boundary condition

$$\eta'_2(x_f) + |k_2|\eta_2(x_f) = 0 \quad (3.14c)$$

at some large distance $x_f > 0$. As a result of these conditions, far from the Q-ball the profile of the first, propagating, component has the form

$$\eta_1(x) = A_{\text{rad}} \cos(k_1|x| + \delta). \quad (3.15)$$

An example of such a symmetric half-propagating solution is presented in figure 5.

The consequences of the excitation of the half-propagating mode are twofold. First, the non-propagating part $\eta_2(x)$ has an impact on the profile of the Q-ball. Second, the

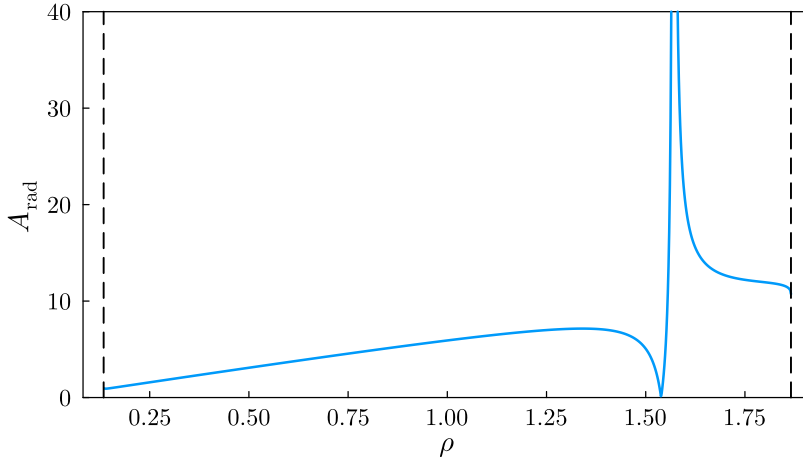


Figure 6. Radiation tails of the symmetric half-propagating modes as a function of ρ for $\beta = \frac{1}{4}$ and $\omega = \frac{\sqrt{3}}{2}$.

propagating component of this mode $\eta_1(x)$ radiates away the energy of the perturbed configuration. We can expect that the modes with the largest amplitude would decay faster, and conversely, the modes with the smallest amplitude would stay longer. In figure 6 we show the amplitude A_{rad} of the propagating component as a function of ρ for $\beta = \frac{1}{4}$ and $\omega = \frac{\sqrt{3}}{2}$. There are two important features. First, around $\rho = 1.57$ this amplitude grows almost to infinity, which indicates that our boundary conditions (3.14) cannot be simultaneously fulfilled, which basically means that $\eta_2(0)$ should vanish. Second, before this discontinuity, the amplitude of the propagating mode becomes very small, $A_{\text{rad}} = 0.0034979$ for $\rho = 1.538789$. Such a minimal radiation tail can, and in this case does, indicate the presence of a quasinormal mode [20]. Quasinormal modes satisfy purely outgoing boundary conditions, which break the Hermiticity of the operator L in (3.4). This allows the eigenfrequency to be complex. And indeed, we have found a quasinormal mode at $\rho = 1.538789 + 1.180 \cdot 10^{-5}i$. The half-life of this mode is $T_{1/2} = \frac{1}{\text{Im} \rho} \log(2) \approx 58700$ which explains the longevity of the oscillations. The profile of the half-propagating mode with minimal radiation tail is shown in figure 7.

3.4 Bound modes

For perturbation frequencies $\rho \in (0, 1 - \omega)$ neither of the components can propagate, and the profiles have only exponential tails. The corresponding normalizable modes are bound to the Q-ball. We found various examples of these modes, including¹ in the case $\beta = 0$ analysed in [9]. As mentioned above, there always is a translational zero mode and one bound mode for $\rho = 0.1336$, which is very close to the frequency of one of the peaks in the spectrum. The component for $\omega - \rho$ is localized at $x = 0$, the other $\omega + \rho$ is very close to

¹For most of our analysis we consider stable Q-balls with $\beta \geq \frac{1}{4}$, but we devote Appendix A to the relaxation problem for $\beta = 0$.

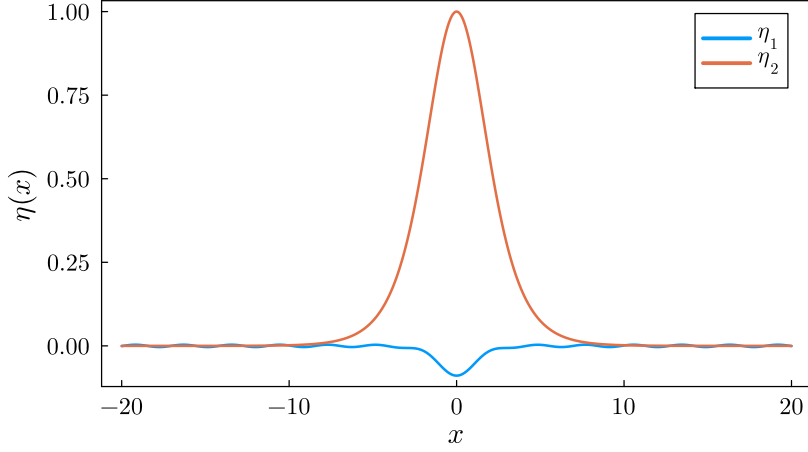


Figure 7. profile of the half-propagating mode with minimal radiation tail for $\beta = \frac{1}{4}$ and $\omega = \frac{\sqrt{3}}{2}$ and $\rho = 1.538789$.

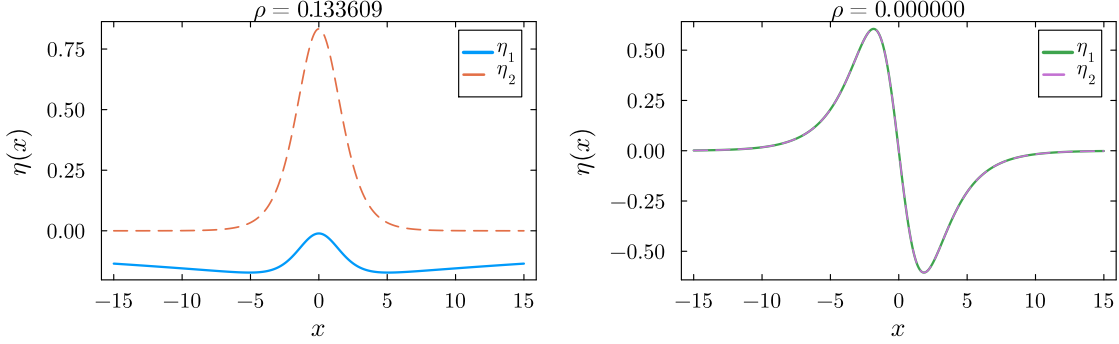


Figure 8. Bound modes for $\beta = \frac{1}{4}$ and $\omega = \frac{\sqrt{3}}{2}$.

the threshold, but $\eta_2(0)$ is much smaller than $\eta_1(0)$, which explains why there is no peak near the threshold in the power spectrum of $\phi(0, t)$.

For $\beta = \frac{1}{4} + \epsilon$ the Q-ball frequency can be small and the Q-ball profile looks like two weakly bound kinks. In the spectrum there are two modes that can be interpreted as symmetric and antisymmetric combinations of translational modes of the kinks. The symmetric combination, which has frequency $\rho = 0$, is the translational mode of the Q-ball. The antisymmetric combination, with $\rho > 0$, represents the oscillation of the width of the Q-ball. Moreover, as seen on the right-hand side of figure 9, more modes appear as $\omega \rightarrow 0$, since the potential generated by the Q-ball has a wide well, which can support many modes. An example of such a case is shown in figure 10.

3.5 Mode decay

Considering perturbations of the Q-ball we repeat the same procedure as in [9], i.e. we examine a one-parameter squashing/stretching perturbation of the form

$$\phi \rightarrow \phi_\lambda = \sqrt{\lambda} e^{i\omega t} f(\lambda x), \quad (3.16)$$

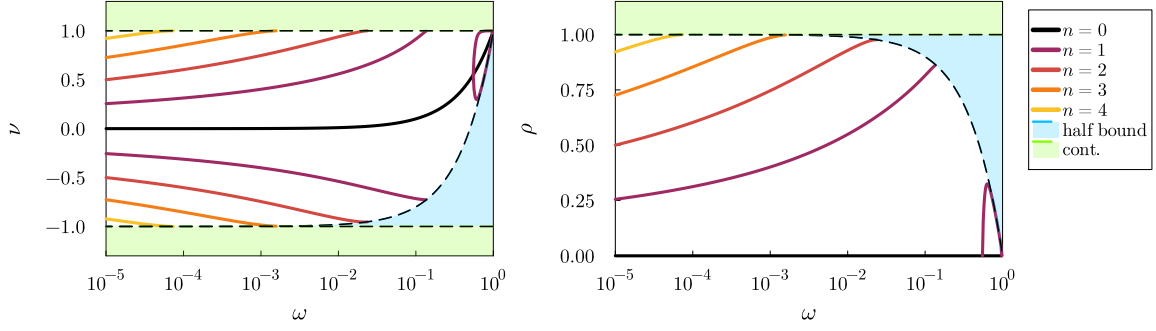


Figure 9. Eigenfrequencies of bound modes for $\beta = 1/4$ as a function of ω .

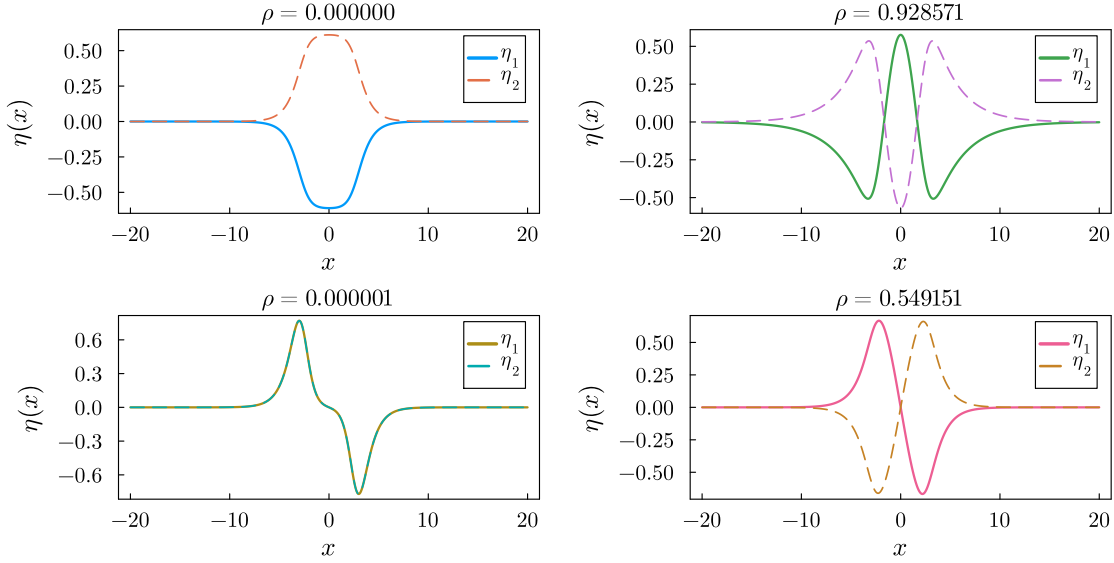


Figure 10. Bound modes of a small frequency Q-ball $\beta = 1/4$, $\omega = 0.01$.

where λ is a positive parameter. Note that these deformations do not affect the charge of the Q-ball. Hereafter we consider the most interesting case of a twofold degenerate vacuum and take $\beta = \frac{1}{4}$, $\lambda = 1.05$ and $\omega = \frac{\sqrt{3}}{2}$. The decay of the perturbation is shown in Fig. 11. In the Appendix we present and comment on a similar plot for the $\beta = 0$ case studied in [9]. Considering the longer time evolution of the initially squashed Q-ball, we see that the perturbation decays with time, although the decay rate slows down. However, there is a pattern, which is similar to the Manton-Merabet law [36] for the decay of the shape mode of the ϕ^4 kink: $A(t) \sim t^{-1/2}$.

In Figure 12 we show the power spectra of the field ϕ at the centre and at $x = 10$, and, following [9], the power spectrum of the magnitude of the field $|\phi(0, t)|$. Both the spectra of the field values and of their absolute values carry valuable information. Below we examine explicitly what are the differences between these two approaches.

Let us suppose that the field can be represented as a sum of modes oscillating with

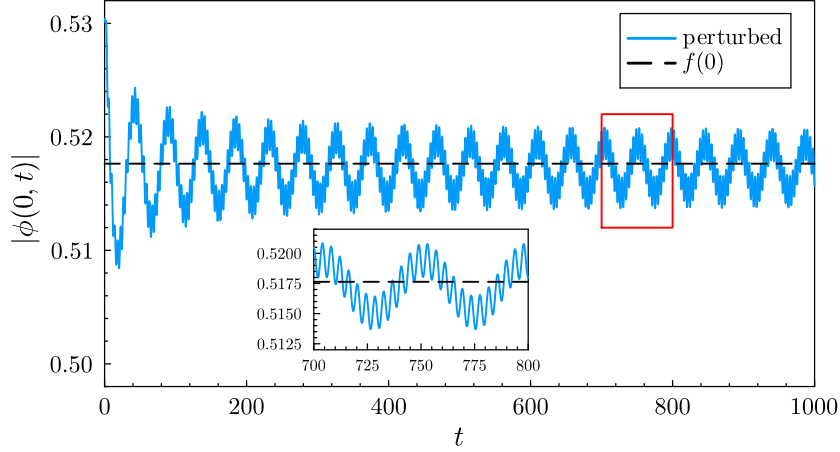


Figure 11. Evolution of the amplitude of the perturbed Q-ball $|\phi(0, t)|$ at the centre of the configuration for $\beta = \frac{1}{4}$, $\omega = \frac{\sqrt{3}}{2}$ and $\lambda = 1.05$.

frequencies ν_n :

$$\phi(0, t) \approx \sum_n c_n e^{i\nu_n t}. \quad (3.17)$$

This yields

$$|\phi(0, t)|^2 = \phi\phi^* \approx \sum_{n,m} c_n c_m^* e^{i(\nu_n - \nu_m)t}. \quad (3.18)$$

Thus, there are configurations with the same absolute value of the field $|\phi(0, t)|$ but different frequencies.

First, we consider the features of the power spectrum of perturbations at the center of the Q-ball, see the blue curve in Figure 12. The most prominent peaks in the spectrum correspond to the frequencies (in ascending order) -0.673 , 0.734 , 0.866 and 2.405 .

- Clearly, the highest peak at $\nu = 0.866$ corresponds to the frequency of the stationary Q-ball, $\omega = \sqrt{3}/2$.
- The peak at $\nu = 0.734$ corresponds to the oscillational mode with $\nu = \omega - \rho_1$ with $\rho_1 = 0.1336$.
- At $\nu = \omega + \rho_1 = 0.9996 < 1$ there is a peak (barely visible at $x = 0$ but quite prominent at $x = 10$ - red dashed line) corresponding to the second frequency of the mode. Although $\nu = \omega + \rho_1$ is very close to 1 it is easy to verify numerically that it is still below the threshold, see figure 8.
- The peak at $\nu = -0.673$ corresponds to the lower real part of the quasinormal mode with the real part of the frequency $\rho_2 = 1.539$.
- The second frequency of the quasinormal mode, corresponding to the propagating component, is visible at $\nu = \omega + \rho_2 = 2.405$.

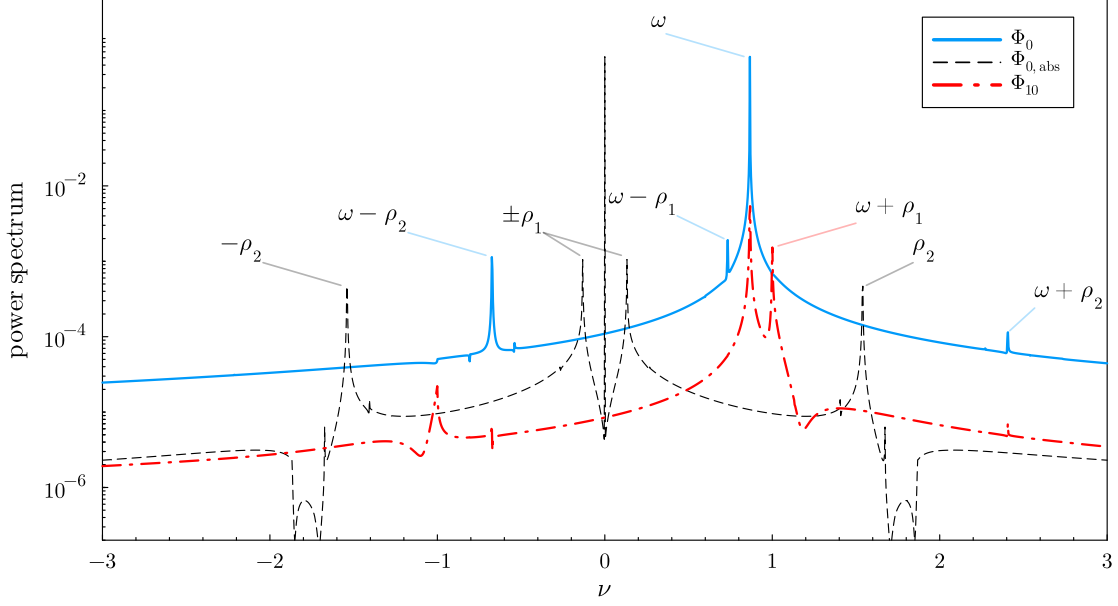


Figure 12. Power spectra of the fluctuations of the field ϕ (blue solid line) and of its absolute value $|\phi|$ (black dashed line) at the origin $x = 0$, and of the field ϕ at $x = 10$ (dash-dotted red line), all with $\beta = \frac{1}{4}$.

The mode $\omega - \rho_1$ is bounded while the mode $\omega - \rho_2$ is half-propagating. Indeed, considering the power spectrum of fluctuations at $x = 10$, see the red dash-dotted curve in Figure 12, we can clearly identify the Q-ball frequency ω and threshold frequencies ± 1 . Also, small peaks at $\omega \pm \rho_2$ are visible there.

The power spectrum of fluctuations of absolute value of the field at the origin is displayed in Figure 12, black curve. The most prominent peak is at $\omega = 0$ which corresponds to the net contribution of all frequencies, $\omega_n - \omega_n = 0$. Another peak, at ± 0.132 , corresponds to $\pm(\omega_3 - \omega_2)$ and the peaks at ± 1.541 correspond to $\pm(\omega_3 - \omega_1)$.

4 Radiation pressure

In this section, we investigate how Q-balls move when exposed to scalar radiation. We expect that for small amplitudes (much smaller than the amplitude of the Q-ball) the waves would scatter according to linearized equations. The scattered waves can have different momenta than the initial wave, and the excess of the momentum carried by waves can be related to the force acting on the Q-ball. In particular, we will show that the radiation can both push (positive radiation pressure, PRP) or pull (negative radiation pressure, NRP) the Q-ball depending on the composition of the incoming wave.

Following [31, 32], let us consider a field within a finite interval $x \in [-L, L]$, where $L \gg 1$, containing a Q-ball and a wave scattered off the Q-ball. The total momentum of

the field in this interval is given by

$$P = \int_{-L}^L \mathcal{P} dx = - \int_{-L}^L T_{tx} dx = - \int_{-L}^L (\phi_t \phi_x^* + \phi_t^* \phi_x) dx, \quad (4.1)$$

where \mathcal{P} is the momentum density, and T is the energy-momentum tensor. A moving Q-ball then has momentum $P = E\gamma v$. A wave scattered off the Q-ball carries momentum which can be obtained from the conservation law $\partial_\mu T^{\mu\nu} = 0$

$$\partial_t \mathcal{P} = -\partial_x T_{xx} = -\partial_x [\partial_t \phi \partial_t \phi^* + \partial_x \phi \partial_x \phi^* - V(|\phi|^2)]. \quad (4.2)$$

Integrating the left-hand side of the above expression and averaging over a period gives the rate of change of the momentum within the interval. The right hand is a total derivative, so integration gives only boundary terms. Assuming that the wave asymptotically (for $x \approx \pm L$) has the form $\phi = A(x)e^{i(\nu t - kx)}$, where $A(x)$ is a slowly changing function, we find that the rate of change of the momentum inside of the interval is equal to the flux of momentum through the boundaries of the interval:

$$\frac{dP}{dt} = \int_{-L}^L \partial_t \mathcal{P} dx = 2k^2 [A^2(-L) - A^2(L)]. \quad (4.3)$$

Assuming that the amplitudes of the waves are small compared to that of the Q-ball, we can identify $\frac{dP}{dt}$ as a force F acting on the Q-ball.

A single mode consists of two components with frequencies $\nu_1 = \omega + \rho$ and $\nu_2 = \omega - \rho$. Therefore, the asymptotic form of the field for which the incident wave propagates in channel j is

$$\phi(x \rightarrow -\infty) = A \sum_{l=1,2} (\delta_{lj} + r_j) e^{i(\nu_l t + k_l x)} \quad (4.4)$$

$$\phi(x \rightarrow \infty) = A \sum_{l=1,2} t_l e^{i(\nu_l t - k_l x)} \quad (4.5)$$

The rate of momentum transfer to the Q-ball is the sum of contributions coming from all scattered waves:

$$F_j = 2A^2 \sum_{l=1,2} k_l^2 (\delta_{lj} + R_l - T_l) \quad (4.6)$$

where $R_l = |r_l|^2$ and $T_l = |t_l|^2$ are reflection and transmission coefficients in each channel and k_l are wave numbers. Negative radiation pressure can occur if the transmission coefficient from a smaller to larger wave number channel is large enough. The only such scenario is when the incident wave corresponds to a frequency $\nu_2 = \omega - \rho < -1$. The other frequency is equal to $\nu_1 = 2\omega - \nu_2$, so $|k_2| < |k_1|$. Figure 13 shows the force calculated from the solution of the linearized equation exactly in such a case. For values of $|\nu_2|$ close to the threshold positive radiation pressure is expected, while for larger $|\nu_2|$ there are regions where negative radiation pressure should be visible. The red colour represents PRP and the blue, NRP. In the other case, with an incident wave in the first component, the radiation pressure was always positive. An example of both positive and negative radiation pressure for $\beta = 0.26$ and $\omega = 0.4$ is shown in figure 14. The accelerations predicted from the

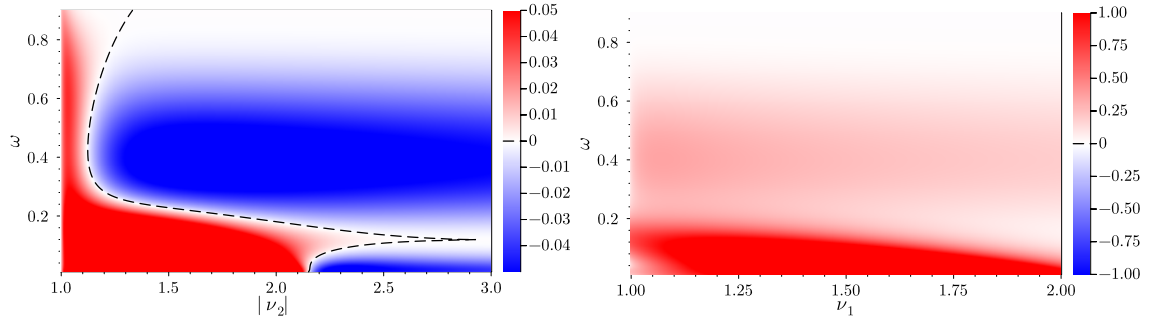


Figure 13. Force (divided by A^2) exerted on Q-balls for $\beta = \frac{1}{4}$ as a function of ν_2 and ω in the case of incident wave in the second sector.

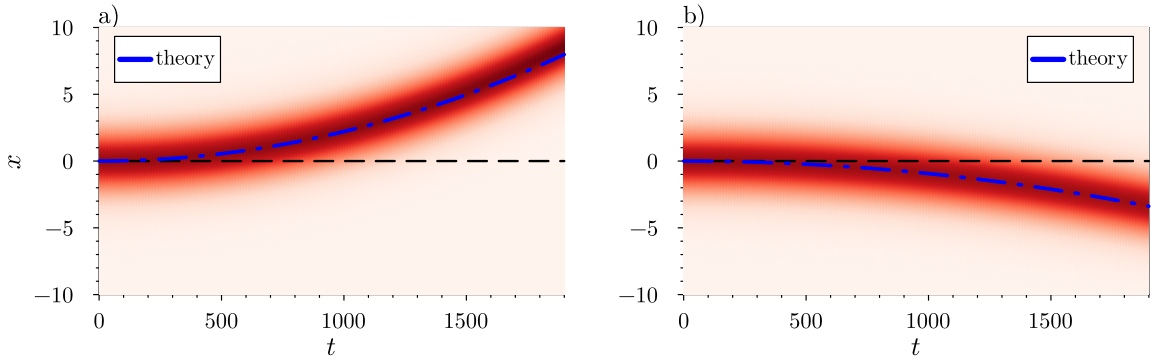


Figure 14. Motion of Q-balls under the influence of a wave in a) first channel and b) second channel. $\beta = 0.26$, $\omega = 0.6$, $\rho = 2.1$, $A = 0.01$. Colour intensity indicates the amplitude of the field.

effective force (4.6) agree well with the accelerations computed from numerical simulations of the full PDE, as presented in figure 15.

In the same way as we calculated the force from the energy and momentum conservation law, we can calculate the rate of change of the charge of a Q-ball by integrating (2.3)

$$\frac{dQ}{dt} = \int dx \partial_x j_x = 2A^2 \sum_{l=1,2} |k_l| (\delta_{lj} - R_l - T_l) \quad (4.7)$$

Numerically we found this value to be of order 10^{-15} , which means that to linear order the wave does not change the charge of the Q-ball. The result is not surprising because it follows from the unitarity of the S matrix.

5 Conclusions

In this paper we have discussed how external perturbations affect Q-balls in (1+1) dimensions. Two examples are considered: (i) squashing perturbations of the Q-ball and (ii) interaction with incoming radiation. Considering the power spectrum of linearized perturbations about the Q-ball we find that there are both translational and phase shifting zero modes, as well as bounded, half-propagating and quasi-normal modes. We have shown

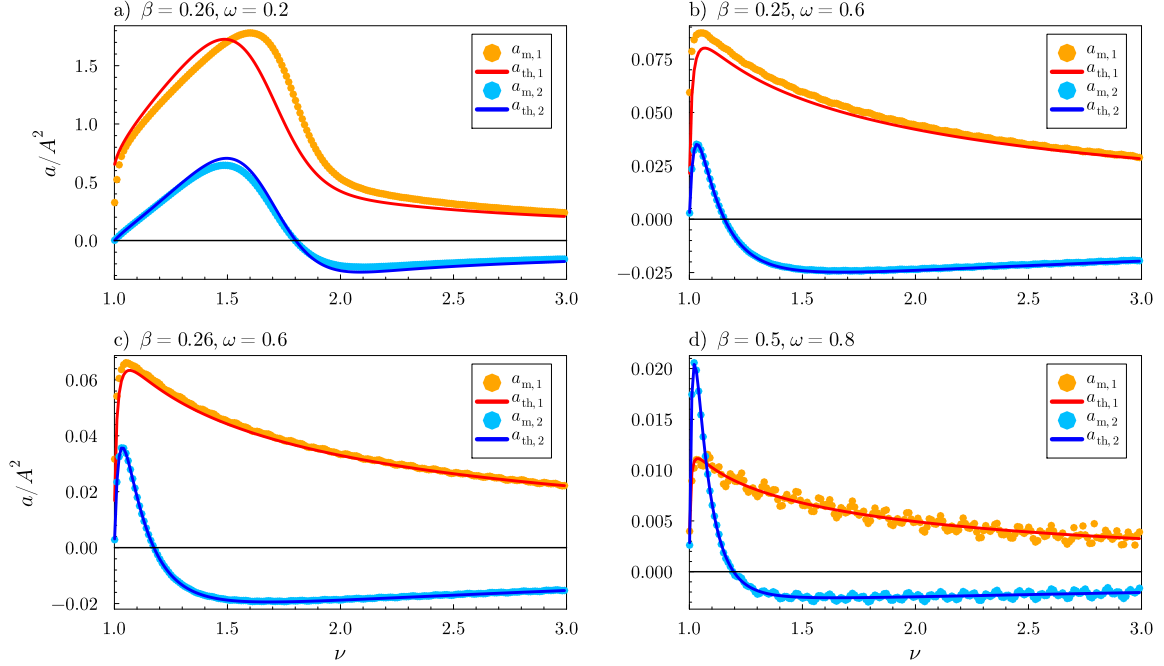


Figure 15. Comparison of measured acceleration (dots) with theoretical prediction (lines).

that, depending on the nature of the incoming wave, the Q-ball can be pulled towards the source of the incident radiation, or it can be pushed away from it.

An interesting extension of this work would be to study perturbative excitations of Q-balls in (3+1) dimensions. Another interesting question, which we hope to be addressing in the near future, is to investigate the decays of Q-balls caused by external perturbations.

We note, finally, that stationary rotating Q-balls can induce superradiant amplification for scattered outgoing waves [37]. An important assumption in [37] is that the incoming wave does not excite the translational mode of the Q-ball. As a result its position does not change during the process of superradiant emission of radiation, related to the resonance energy transfer from the stationary Q-ball to the scattered wave. However, since, as we have seen, radiation pressure on the Q-ball pushes it to move, one may wonder whether this will affect the criteria for superradiance to occur, and it would be interesting to investigate this question further.

Acknowledgements

PED was supported in part by the STFC under consolidated grant ST/T000708/1 “Particles, Fields and Spacetime”, and would like to thank the African Institute for Mathematical Sciences, South Africa, for hospitality during the last stages of this work. TR was supported by the Polish National Science Center, grant NCN 2019/35/B/ST2/00059. TR and DC were supported by the Priority Research Area under the program Excellence Initiative—Research University at the Jagiellonian University in Kraków. YS would like to thank the Hanse-Wissenschaftskolleg Delmenhorst for support. We would like to thank

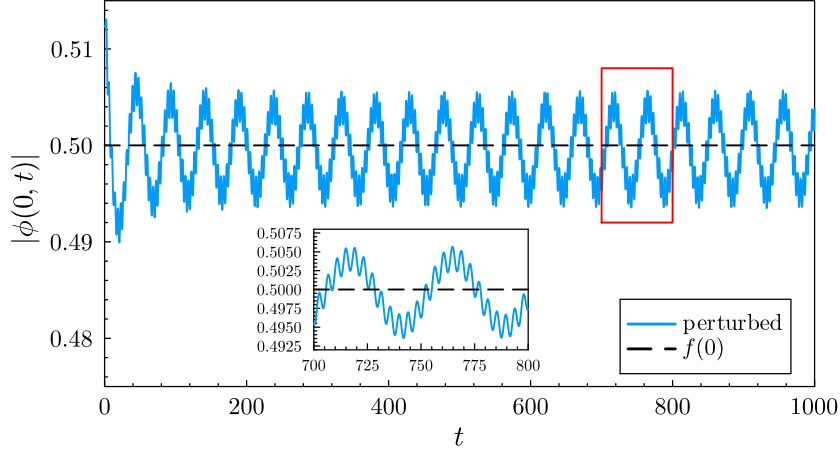


Figure 16. Evolution of the amplitude of the perturbed Q-ball $|\phi(0, t)|$ at the centre of the configuration for $\beta = 0$, $\omega = \frac{\sqrt{3}}{2}$ and $\lambda = 1.05$.

Mikhail Smolyakov for pointing out the presence of the Lorentz mode, which was missed in the previous version of the manuscript.

A Metastable Q-balls

In the main part of this paper we studied the behavior of Q-balls for models with $\beta \geq \frac{1}{4}$, when potentials have one ($\phi = 0$ for $\beta > \frac{1}{4}$) or two vacua ($|\phi| = 0, \sqrt{2}$ for $\beta = \frac{1}{4}$). For $\beta < \frac{1}{4}$ the minimum at $\phi = 0$ is just a local minimum, and therefore it is a false vacuum. However, certain restricted configurations, if not excited too much, can exist around the false vacuum, at least in the classical theory. In [9] the decay of such a configuration for the model with $\beta = 0$ was discussed. We have repeated the same analysis as in section 3.5 but for $\beta = 0$. In this appendix we report on these results.

We present the decay in figure 16, while the power spectra are presented in figure 17. A direct comparison with figure 12 shows a very similar spectral structure with a single bound and one quasi-normal mode. The bound mode is for $\rho_1 = 0.1317$ and the QNM is for $\rho_2 = 1.5150692 + 9.96 \cdot 10^{-5}i$. Measured peaks: -0.650, 0.731, 0.997, 2.383 are consistent with the bound mode $\omega + \rho_1 = 0.9977$, $\omega - \rho_1 = 0.7343$ and the QNM $\omega + \text{Re } \rho_2 = 2.3811$ and $\omega - \text{Re } \rho_2 = -0.64904$. In [9] the authors claim that the persisted oscillations are due to the bound state of two Q-balls, some form of a breather. However, since the frequencies match so well with the bound and the quasinormal mode, we believe that their claim is overstated.

References

- [1] G. Rosen, *Particlelike Solutions to Nonlinear Complex Scalar Field Theories with Positive-Definite Energy Densities*, *J. Math. Phys.* **9** (1968) 996.

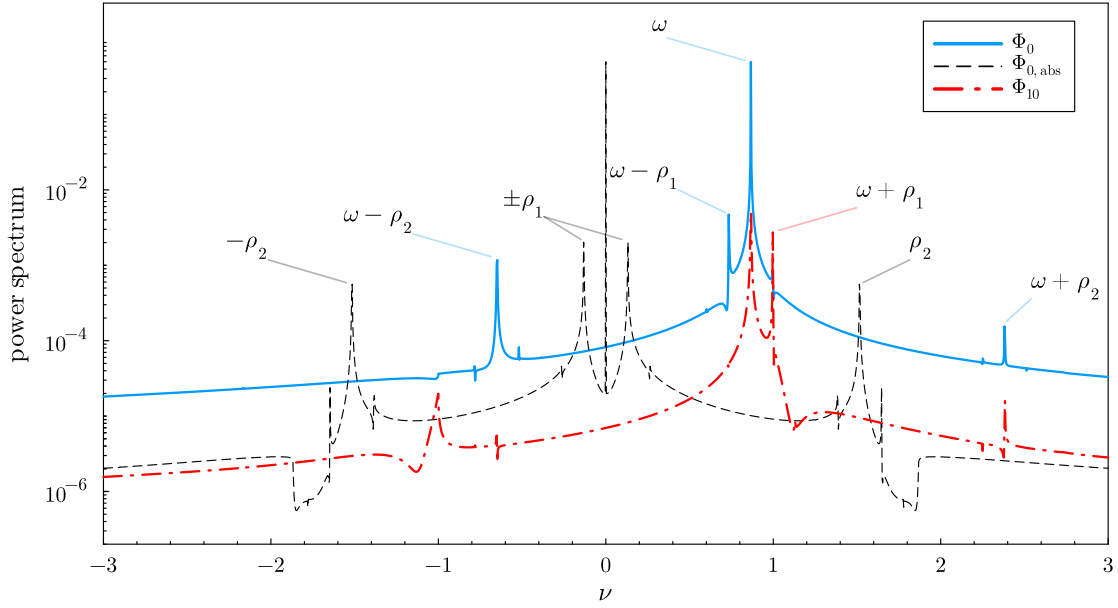


Figure 17. Power spectra of the fluctuations of the field ϕ (blue solid line) and of its absolute value $|\phi|$ (black dashed line) at the origin $x = 0$, and of the field ϕ at $x = 10$ (dash-dotted red line), all with $\beta = 0$.

- [2] R. Friedberg, T. D. Lee and A. Sirlin, *A Class of Scalar-Field Soliton Solutions in Three Space Dimensions*, *Phys. Rev. D* **13** (1976) 2739–2761.
- [3] S. R. Coleman, *Q-balls*, *Nucl. Phys. B* **262** (1985) 263.
- [4] T. D. Lee and Y. Pang, *Nontopological solitons*, *Phys. Rept.* **221** (1992) 251–350.
- [5] E. Radu and M. S. Volkov, *Existence of stationary, non-radiating ring solitons in field theory: knots and vortons*, *Phys. Rept.* **468** (2008) 101–151, [[0804.1357](#)].
- [6] Y. M. Shnir, *Topological and Non-Topological Solitons in Scalar Field Theories*. Cambridge Monographs on Mathematical Physics. Cambridge University Press, 2018, [10.1017/9781108555623](#).
- [7] M. Axenides, S. Komineas, L. Perivolaropoulos and M. Floratos, *Dynamics of nontopological solitons: Q balls*, *Phys. Rev. D* **61** (2000) 085006, [[hep-ph/9910388](#)].
- [8] R. Battye and P. Sutcliffe, *Q-ball dynamics*, *Nucl. Phys. B* **590** (2000) 329–363, [[hep-th/0003252](#)].
- [9] P. Bowcock, D. Foster and P. Sutcliffe, *Q-balls, integrability and duality*, *Journal of Physics A: Mathematical and Theoretical* **42** (2009) 085403.
- [10] E. J. Copeland, P. M. Saffin and S.-Y. Zhou, *Charge-Swapping Q-balls*, *Phys. Rev. Lett.* **113** (2014) 231603, [[1409.3232](#)].
- [11] S. Chandrasekhar and S. Detweiler, *The quasi-normal modes of the Schwarzschild black hole*, *Proceedings of the Royal Society of London. A. Mathematical and Physical Sciences* **344** (1975) 441–452.

- [12] K. D. Kokkotas and B. G. Schmidt, *Quasinormal modes of stars and black holes*, *Living Rev. Rel.* **2** (1999) 2, [[gr-qc/9909058](#)].
- [13] R. A. Konoplya and A. Zhidenko, *Quasinormal modes of black holes: From astrophysics to string theory*, *Rev. Mod. Phys.* **83** (2011) 793–836, [[1102.4014](#)].
- [14] P. Forgács and M. S. Volkov, *Resonant excitations of the 't Hooft–Polyakov monopole*, *Phys. Rev. Lett.* **92** (Apr, 2004) 151802.
- [15] E. Ching, P. Leung, A. M. Van Den Brink, W. Suen, S. Tong and K. Young, *Quasinormal-mode expansion for waves in open systems*, *Reviews of Modern Physics* **70** (1998) 1545.
- [16] M. N. Smolyakov, *Perturbations against a Q-ball: Charge, energy, and additivity property*, *Phys. Rev. D* **97** (2018) 045011.
- [17] I. L. Bogolyubsky and V. G. Makhankov, *On the Pulsed Soliton Lifetime in Two Classical Relativistic Theory Models*, *JETP Lett.* **24** (1976) 12.
- [18] E. J. Copeland, M. Gleiser and H. R. Muller, *Oscillons: Resonant configurations during bubble collapse*, *Phys. Rev. D* **52** (1995) 1920–1933, [[hep-ph/9503217](#)].
- [19] M. Gleiser, *Pseudostable bubbles*, *Phys. Rev. D* **49** (1994) 2978–2981, [[hep-ph/9308279](#)].
- [20] G. Fodor, P. Forgacs, P. Grandclement and I. Racz, *Oscillons and Quasi-breathers in the ϕ^4 Klein-Gordon model*, *Phys. Rev. D* **74** (2006) 124003, [[hep-th/0609023](#)].
- [21] G. Fodor, P. Forgacs, Z. Horvath and M. Mezei, *Computation of the radiation amplitude of oscillons*, *Phys. Rev. D* **79** (2009) 065002, [[0812.1919](#)].
- [22] P. Grandclement, G. Fodor and P. Forgacs, *Numerical simulation of oscillatons: extracting the radiating tail*, *Phys. Rev. D* **84** (2011) 065037, [[1107.2791](#)].
- [23] E. P. Honda and M. W. Choptuik, *Fine structure of oscillons in the spherically symmetric ϕ^4 Klein-Gordon model*, *Phys. Rev. D* **65** (2002) 084037, [[hep-ph/0110065](#)].
- [24] P. Dorey, T. Romanczukiewicz and Y. Shnir, *Staccato radiation from the decay of large amplitude oscillons*, *Phys. Lett. B* **806** (2020) 135497, [[1910.04128](#)].
- [25] H.-Y. Zhang, M. A. Amin, E. J. Copeland, P. M. Saffin and K. D. Lozanov, *Classical Decay Rates of Oscillons*, *JCAP* **07** (2020) 055, [[2004.01202](#)].
- [26] S. Kasuya, M. Kawasaki and F. Takahashi, *I-balls*, *Phys. Lett. B* **559** (2003) 99–106, [[hep-ph/0209358](#)].
- [27] M. Kawasaki, F. Takahashi and N. Takeda, *Adiabatic Invariance of Oscillons/I-balls*, *Phys. Rev. D* **92** (2015) 105024, [[1508.01028](#)].
- [28] D. G. Levkov, V. E. Maslov, E. Y. Nugaev and A. G. Panin, *An Effective Field Theory for large oscillons*, *JHEP* **12** (2022) 079, [[2208.04334](#)].
- [29] T. Romanczukiewicz, *Interaction between kink and radiation in ϕ^4 model*, *Acta Phys. Polon. B* **35** (2004) 523–540, [[hep-th/0303058](#)].
- [30] T. Romanczukiewicz, *Negative radiation pressure in case of two interacting fields*, *Acta Phys. Polon. B* **39** (2008) 3449–3462, [[0807.2314](#)].
- [31] P. Forgacs, A. Lukacs and T. Romanczukiewicz, *Negative radiation pressure exerted on kinks*, *Phys. Rev. D* **77** (2008) 125012, [[0802.0080](#)].

- [32] D. Ciurla, P. Forgács, A. Lukács and T. Romańczukiewicz, *Negative radiation pressure in Bose-Einstein condensates*, *Phys. Rev. E* **109** (Jan, 2024) 014228.
- [33] P. Dorey, A. Gorina, T. Romańczukiewicz and Y. Shnir, *Collisions of weakly-bound kinks in the Christ-Lee model*, *JHEP* **09** (2023) 045, [[2304.11710](#)].
- [34] M. A. Lohe, *Soliton Structures in $P(\phi)$ in Two-dimensions*, *Phys. Rev. D* **20** (1979) 3120.
- [35] M. N. Smolyakov, *Perturbations against a Q -ball. II. contribution of nonoscillation modes*, *Phys. Rev. D* **100** (Aug, 2019) 045002.
- [36] N. S. Manton and H. Merabet, *ϕ^4 kinks - gradient flow and dynamics*, *Nonlinearity* **10** (1997) 3.
- [37] P. M. Saffin, Q.-X. Xie and S.-Y. Zhou, *Q -ball superradiance*, *Phys. Rev. Lett.* **131** (Sep, 2023) 111601.